MAX-PLANCK-INSTITUT FÜR PLASMAPHYSIK

GARCHING BEI MÜNCHEN

NUMERICAL CALCULATIONS OF LOCALIZED IDEAL AND RESISTIVE INSTABILITIES IN INTOR EQUILIBRIA

D. CORREA-RESTREPO

IPP 6/272 December 1987

Die nachstehende Arbeit wurde im Rahmen des Vertrages zwischen dem Max-Planck-Institut für Plasmaphysik und der Europäischen Atomgemeinschaft über die Zusammenarbeit auf dem Gebiete der Plasmaphysik durchgeführt.

Abstract

The stability of typical INTOR equilibria with respect to localized ideal and resistive instabilities is investigated. Configurations which are stable to ideal ballooning modes (and are therefore also Mercier stable) are shown to be unstable with respect to resistive ballooning instabilities, and the corresponding growth rates are calculated. A useful relation is given which allows calculation of the resistive growth rate at the ideal ballooning limit. This relation is also valid for three-dimensional equilibria.

1. Introduction

The ideal MHD stability propertities and beta limits of tokamak plasma configurations which model INTOR equilibria have previously been investigated by several authors, e.g. $[1-7]$. These calculations describe the behaviour of the plasma with respect to both external and internal modes and lead to the conclusion that the beta limit is approximately given by the well-known scaling law [8] $\beta_c(\%) = gJ_N$, $J_N = \mu_0 J_p \,/\, aB_0$. Here, β_c is the critical beta, μ_0 is the permittivity of the vacuum , J_p is the total plasma current, a is the horizontal minor plasma radius, B_0 is the magnetic induction on axis and g is a constant which takes a value in the range of approx. 3 to 4.

Up to now, most attention has been devoted to the investigation of ideal MHD modes, and dissipative effects have largely been neglected . Nevertheless, it is known that the presence of electrical resistivity can deteriorate the stability properties of an otherwise ideally stable plasma $[9-11]$. In particular, the calculations done near the magnetic axis for a very simple model of a tokamak with a circular plasma cross-section [12, 13] show that high-n resistive ballooning modes appear in the first region of ideal stability and shift the stability boundaries toward lower values of beta. In this model, resistive interchanges and resistive ballooning modes also appear in the second region of ideal stability. This makes it somewhat uncertain whether advantage can be taken of the good stability propertities at high beta values in the second ideally stable region. Using a different model, other authors [14] believe that resistive ballooning modes are of no importance in the second ideally stable region. However, it should be considered that these conclusions are obtained by employing the usual method of matching asymptotic solutions of differential equations, and that this method, in its usual form (which takes into account only lowest-order expressions in a certain expansion), is in general not applicable in the second region of stability [12].

Here, attention is limited to the first region of stability, in which the properties of a

typical INTOR plasma with respect to localized resistive modes are studied.

It should be noted that, although the calculations are done with equilibrium parameters appropriate to INTOR configurations, the results are relevant to other tokamaks as well, the main feature being the reduction of β_c as a consequence of resistive ballooning effects. This had already been established in [12, 13]and was also verified later by other authors using different numerical methods [19]. The following result has an even wider range of applications, including three-dimensional configurations: if the equilibrium is at marginal stability for ideal ballooning modes, it is unstable with respect to resistive ballooning modes. The corresponding resistive growth rate is given by a simple expression already derived in [10, 11] and introduced here in Section 3.2. This fact agrees with observations made in ASDEX discharges, where resistive ballooning instabilities at the ideal β limit are believed to be responsible for enhanced energy losses [20].

Section 2 describes the geometrical parameters and the two arbitrary surface functions which enter the equilibrium calculations. Section 3 presents the stability calculations, and Section 4 the conclusions. Finally, in the Appendix, useful expressions are given for the surface quantities which appear in the stability calculations.

2. Equilibrium

2.1 Description of the geometry

Let R, ϕ, z be the usual cylindrical coordinates. The axis of symmetry of the system is then described by $R = 0$. In addition to these coordinates, a poloidal coordinate θ is introduced on the planes $\phi = const.$ and the shape of the plasma cross-section at the surface is taken as

$$z = e\, a \sin\theta \tag{2.1}$$

and

$$R/a = r_0 + r_1 \cos\theta + r_2 \cos 2\theta + r_3 \cos 3\theta + r_4 \cos 4\theta\,, \tag{2.2}$$

with e the ellipticity, a the horizontal minor radius and

$$r_0 = \frac{R_0}{a} - \frac{\delta}{2} + \frac{\delta^3}{16}\,, \tag{2.3}$$

$$r_1 = 1 - \frac{\delta^2}{8}\,, \tag{2.4}$$

$$r_2 = \frac{\delta}{2} - \frac{\delta^3}{12}\,, \tag{2.5}$$

$$r_3 = \frac{\delta^2}{8} \tag{2.6}$$

and

$$r_4 = \frac{\delta^3}{48} \quad . \tag{2.7}$$

The parameter δ describes the triangularity of the boundary and R_0 is the radius of the geometrical centre, i.e.

$$R_0 = (R(\theta = \pi) + R(\theta = 0)) / 2 \quad . \tag{2.8}$$

Thus, the frequently used expression for the radius, namely

$$\frac{R}{a} = \frac{R_0}{a} + \cos (\theta + \delta \sin \theta) \quad , \tag{2.9}$$

and equation (2.2) can be shown to be identical up to terms $\sim \delta^3$. For our purposes, this guarantees perfectly sufficient accuracy in the identification of equations (2.2) and (2.9).

For the calculations, the aspect ratio R_0/a is taken to be 4 , the elongation e is 1.6 and the triangularity δ is 0.3.

2.2 Magnetic field and equilibrium profiles

In the axisymmetric systems considered here , the magnetic field $\mathbf{B}$ is given by

$$\mathbf{B} = \frac{1}{2\pi} \nabla\phi \times \nabla\chi + f \nabla\phi \quad , \tag{2.10}$$

where χ is the poloidal flux and

$$f = (I_0 - I) / 2\pi \quad , \tag{2.11}$$

I being the poloidal current inside the particular surface, and I_0 the total current flowing in the z-direction through a surface encircled by the magnetic axis.

The two arbitrary surface functions chosen here to describe the equilibrium further are - in contrast to other INTOR calculations - not the pressure p and the safety factor q, but the rotational transform $\iota = 1/q$ and the adiabatic invariant $m = p\left(\frac{1}{4\pi^2} \left|\frac{dv}{ds}\right|\right)^{\Gamma}$, both as a function of the normalized *toroidal* flux s, with $s = \Phi/\Phi_b$, Φ being the toroidal magnetic flux, which takes the value Φ_b at the plasma surface. v is the volume enclosed by the surface $s = const.$ and Γ is the ratio of the specific heats, which is taken to be 5/3.

The mass function profile $m(s)$ is given as

$$\frac{m}{m_0} = 1 + c_1 s + c_2 s^2 - (4 + 3c_1 + 2c_2)s^3 + (3 + 2c_1 + c_2)s^4 \quad . \tag{2.12}$$

This form ensures that both p and dp/ds vanish at the plasma surface, as is the case for proposed INTOR pressure profiles [1]. The choice of the constants c_1 and c_2 allows some freedom with the form of the mass profile. The other constant , m_0 , turns out to be - *roughly* - the average beta value.

The rotational transform profile is expressed as

$$\iota = a_0 + a_1 s + a_2 s^2 + a_3 s^3 + a_4 s^4 \quad , \tag{2.13}$$

with the appropiate choice of the coefficients $a_0 - a_4$, so as to resemble INTOR profiles closely.

3. Stability calculations

3.1 Description of the method

For given profiles $m(s)$, $\iota(s)$ and a given shape of the plasma boundary, the equilibrium is calculated by using the axisymmetric version of either the VMEC code [15]or the FIT code [16]. Mercier stability and ideal ballooning stability are investigated - on each surface - with the help of the JMCBALV code [17]. We then proceed to compute, again for each surface, all the average quantities which enter the resistive interchange criterion [9]and the resistive ballooning instability calculations [10-12]. Expressions for these quantities, appropriate to axisymmetric systems and to the coordinates that we use, are given in the Appendix.

The quantity Δ' , which is decisive for ballooning stability, is calculated from the asymptotic solution of the ideal ballooning mode equation. For simplicity, equilibria with up-down symmetry are considered here and Δ' is determined from the *even* solution of the ideal ballooning equation. Calculations done previously for a simple equilibrium [12]showed that even solutions were more unstable than the corresponding uneven ones.

The resistive ballooning mode criterion is evaluated in the relatively simple form derived for the case of large G (G is a quantity given in detail in the Appendix), care being taken not to run into inconsistencies. This means in particular that the growth rates of the instabilities beeing looked for must be larger than a certain critical minimum value. More details about this are given elsewhere [10-12]. In this simple form, the resistive ballooning mode criterion states that there are resistive instabilities with real positive growth rates if the quantity Δ' is positive and exceeds a critical value Δ_c . To calculate Δ_c , one must make assumptions concerning the resistivity and also the degree of localization of the perturbations (which can be described by the mode number n in axisymmetric

systems). Here, we use the Spitzer resistivity , with atomic number $Z = 1$. We take the temperature at the axis to be $15\ keV$ and assume the ion mass to be 2.5 times the mass of the proton, thus corresponding to an ion mixture of 50% helium and 50% tritium. The exact relation between the temperature T and the pressure p is not important for the calculations. We assume here $p \sim T^{3/2}$.

As stated above, the value of Δ_c also depends on the mode number n , for which different arbitrary values are taken. The maximum mode number is also assumed to be limited by the magnitude of the ion gyroradius ρ_i and, for each surface, a maximum allowed mode number is calculated, $n_{max} = r/q\rho_i$, where r is a mean radius and q is, again, the safety factor at the surface under consideration.

The stability of several INTOR equilibria has been calculated, the results for three different, typical cases being shown here

3.2 Resistive growth rate at marginal ideal stability

If a particular surface of the equilibrium under consideration is marginally stable to ideal ballooning modes, then the large asymptotic solution of the ideal ballooning mode equation just vanishes and $|\Delta'| \rightarrow \infty$. From the dispersion relation derived in [10, 11] for $s_M < \frac{1}{2}$, which is valid in any geometry, it is easy to see that this corresponds to a normalized resistive growth rate given by

$$Q^3 = (1 + s_M - H)^2 \quad , \tag{3.1}$$

where s_M (the Mercier exponent) and the quantity H are given explicitly in the Appendix. Thus, the actual growth rate γ scales with resistivity to $1/3$, since Q is defined as

$$Q = \gamma / Q_0 \quad , \tag{3.2}$$

with Q_0 given by equation (A.13).

For an equilibrium which is optimized with respect to ideal ballooning modes, i.e. in which the profiles are such that the ideal ballooning mode equations are marginal at each surface, equation (3.1) is valid over the whole plasma cross-section and allows very easy computation of the resistive growth rate. If only one surface is marginal, equation (3.1) is valid on that surface.

As an example, let us consider an equilibrium calculated with the following profile coefficients:

$$a_0 = 0.909, \quad a_1 = -0.630, \quad a_2 = 0.270, \quad a_3 = 0.131, \quad a_4 = -0.357, \tag{3.3}$$

$$c_1 = -0.305, \quad c_2 = -2.39 \, . \tag{3.4}$$

The other parameters which describe the equilibrium are given in Fig. 1 . Taking different values of m_0 , we find that the equilibrium becomes unstable at the surface $q = 2$ when $m_0 = 0.029$ and $\langle \beta \rangle = 3.01\%$, $\langle \beta \rangle$ being as defined in equation (A.15). The profiles which characterize this equilibrium are given in Fig. 2. The shear and the local poloidal beta are explained at the end of the Appendix. Since the surface under consideration has $s_M = 0.06342$ and $H = 0.0859$, the corresponding normalized growth rate is $Q = 0.9849$. With the parameters given in Fig. 1, the normalization growth rate of equation (A.13) is $Q_0 = (2\pi n)^{2/3} \, 0.665 \cdot 10^3 s^{-1}$. With the help of equation (3.2) it is then easy to calculate the corresponding growth rate γ for different mode numbers n .

If, for instance, $n = 10$,one gets $\gamma^{-1} = 0.951 \cdot 10^{-4} s$. By contrast, the resistive diffusion time is $\tau_R = 1.37 \cdot 10^2 s$ and the Alfvén transit time is $\tau_A = 1.106 \cdot 10^{-6} s$.

3.3 Resistive growth rates below the ideal limit

Below the stability limit to ideal ballooning modes, the parameter Δ' assumes a finite, positive value. The normalized resistive growth rate Q is then obtained from a dispersion relation of the type derived in [10, 11], namely

$$\Delta' = \Delta(Q, \eta, n^2, ...) \quad , \tag{3.5}$$

where Δ is a function of Q , of the resistivity η , of the mode number n , and also of other surface-averaged quantities such as s_M, H, etc... The actual form of Δ depends on the model which is appropriate to the range of Q-values in which one is interested. Thus, if the growth rates we are looking for become very small (i.e. if $Q << 1$), it is indispensable to take into account the stabilizing effect of the sound wave propagation. This leads to a particular form of Δ with -in general- complex solutions for the growth rate Q . For simplicity - and also because it is an interesting situation - the equilibria considered here are not too far away from the ideal marginal limit. More precisely, the growth rates Q of interest are in the approximate range of $0.1 - 1.0$. This is substantially different from other calculations, e. g.those carried out in [18], in which it is assumed that $Q << 1$. Thus, Q can be calculated from the relatively simple form of equation (3.5) which is valid in the case of large G , as already explained above.

The procedure is illustrated by considering an equilibrium calculated with the profiles given by equations (3.3) and (3.4). This equilibrium is known to be marginally stable at $\langle \beta \rangle = 3.01\%$, when $m_0 = 0.029$. With all other parameters left unchanged, but with a lower value of m_0 , namely $m_0 = 0.026$, an equilibrium is calculated which

has $\langle\beta\rangle = 2.70\%$ and which is stable with respect to all localized ideal modes and with respect to resistive interchanges, since $D_R < 0$ everywhere, as can be seen in Fig. 3. Also shown in these diagrams are the Mercier exponent s_M , the magnetic Reynolds number $S = \tau_R/\tau_A$ (with τ_A and τ_R given by equations (A.11) and (A.12) respectively) and the stability parameter Δ' .

As can be seen in Fig. 3, the equilibrium is unstable with respect to resistive ballooning modes ($\Delta' > \Delta_c(n)$). For instance, for a mode number $n = 100$, there is a radial region between $s = 0.68$ and $s = 0.8$ which is unstable. Typical growth rates are $\gamma = 2.5 \cdot 10^3\ s^{-1}$. If one takes the maximum mode numbers which are compatible with the size of the ion gyroradius ($n = 150$ typically), the radial region of instability becomes even larger (from $s = 0.55$ to the surface), the growth rates being in this case $\gamma \approx 3.6 \cdot 10^3\ s^{-1}$.

Fig. 4 shows the profiles and the relevant parameters of another equilibrium. The rotational transform profile is again given by equations (3.3). The mass profile is defined by

$$c_1 = -0.1, \quad c_2 = 0.0\ . \tag{3.6}$$

The corresponding pressure profile is more peaked near the surface than in the preceding examples. The calculations are made with $m_0 = 0.0155$ and $\langle\beta\rangle = 2.0\%$. This equilibrium is stable to all localized ideal modes and to resistive interchanges. As can be seen in Fig. 5, this configuration is also unstable with respect to resistive ballooning modes.

4. Conclusions

The main results of the calculations are now summarized.

For all the cases considered (which are in the first region of ideal stability) resistive interchanges do not appear, since $D_R < 0$ everywhere.

The Mercier exponent s_M is less than 0.5 . The condition for the applicability of a simplified theory of asymptotic matching is thus satisfied in our case.

The results are obtained *without* the restriction that the normalized growth rate Q be small. This makes it possible to study equilibria which are near ideal marginal stability. At the marginal ideal ballooning limit, the equilibria are always resistively unstable, with a normalized growth rate given by $Q = |1 + s_M - H|^{2/3}$. For INTOR configurations, the corresponding inverse growth rates are in the range of milliseconds and are thus faster than resistive processes by a factor of $\sim 10^6$.

Below the ideal marginal limit, the equilibria are also unstable. The corresponding resistive ballooning modes have still considerable growth rates (γ^{-1} also of the order of milliseconds) at values of $\langle\beta\rangle$ that are 80 - 90% of the critical value.

Acknowledgement

The author is grateful to J. Nührenberg, R. Zille and U. Schwenn for providing him with and introducing him to the codes for the equilibrium and ideal stability calculations.

APPENDIX

Equilibrium quantities and scale factor needed to evaluate the resistive ballooning mode criterion in axisymmetric systems

There are several surface-averaged quantities, namely H, E, F^*, D_R etc., which enter the resistive ballooning mode criterion and which are defined in detail elsewhere, e.g. in [10, 11]. Here, appropriate expressions are given to calculate them in axisymmetric systems and in the coordinates used in this paper.

Let s be the normalized toroidal flux introduced in Section 2 and let θ_p and θ_t be appropriately defined poloidal and toroidal coordinates, respectively. If $\sqrt{g}$ denotes the corresponding functional determinant of this coordinates system, then the surface element dS_s of a surface $s = const.$ is given by $dS_s = \sqrt{g}(s,\theta_p)d\theta_p d\theta_t$. Because of the symmetry, there is no dependence on θ_t . The surface average $\langle W \rangle$ of a quantity W is then given by

$$\begin{aligned} \langle W \rangle &= \frac{\int\int W dS_s}{\int\int dS_s} \\ &= \frac{\int\int W\sqrt{g}(s,\theta_p)\ d\theta_p d\theta_t}{\int\int \sqrt{g}(s,\theta_p)\ d\theta_p d\theta_t} \quad . \end{aligned} \tag{A.1}$$

The quantities H, E and F^* can then be expressed as

$$H = \frac{p'v'}{q'\chi'^3}\ 2\pi f \left[\left\langle \frac{1}{|\nabla s|^2}\right\rangle - \frac{1}{\langle B^2\rangle}\left\langle \frac{B^2}{|\nabla s|^2}\right\rangle\right] \quad , \tag{A.2}$$

$$E = \frac{p'v'}{q'\chi'^3}\left\langle \frac{B^2}{|\nabla s|^2}\right\rangle\left[\ \frac{2\pi f}{\langle B^2\rangle} + \frac{v'\chi'' - \chi' v''}{q'\chi'^2}\ \right] \quad , \tag{A.3}$$

$$F^* = \left(\frac{p'v'}{q'\chi'^3}2\pi f\right)^2\left[\left\langle\frac{B^2}{|\nabla s|^2}\right\rangle\left(\frac{\chi'^2}{(2\pi f)^2}\left\langle\frac{1}{B^2}\right\rangle + \left\langle\frac{1}{|\nabla s|^2B^2}\right\rangle\right) - \left\langle\frac{1}{|\nabla s|^2}\right\rangle^2\right] \quad . \quad (A.4)$$

Here, v is the volume enclosed by the surface $s = const.$ and primes denote derivatives with respect to s. In particular, because of the definition of v, one has

$$v' = \int\int \sqrt{g}(s,\theta_p)\; d\theta_p d\theta_t \quad , \qquad (A.5)$$

$$v'' = \int\int \frac{\partial\sqrt{g}(s,\theta_p)}{\partial s} d\theta_p d\theta_t \quad . \qquad (A.6)$$

The quantity D_R, which determines the stability with respect to resistive interchanges, is calculated from the relation

$$D_R = F^* + E + H^2 \quad . \qquad (A.7)$$

The Mercier exponent s_M , which is crucial for Mercier stability, and which also plays an important role in describing the asymptotic behaviour of the ballooning mode equations, is given by

$$s_M = -\frac{1}{2} + \sqrt{(\frac{1}{2} - H)^2 - D_R} \quad . \qquad (A.8)$$

The quantity G of Section 3 is given by

$$G = \frac{\langle B^2\rangle}{p\Gamma M} \quad , \qquad (A.9)$$

with

$$M = \left\langle \frac{B^2}{|\nabla s|^2} \right\rangle \left[\left\langle \frac{|\nabla s|^2}{B^2} \right\rangle + \left(\frac{2\pi f}{\chi'} \right)^2 \left\{ \left\langle \frac{1}{B^2} \right\rangle - \frac{1}{\langle B^2 \rangle} \right\} \right] \quad . \tag{A.10}$$

The evaluation of the resistive ballooning mode criterion also requires calculation of the normalizing growth rate Q_0 and the scale factor y_0, which depend on the resistivity η and on the mode number n. If the Alfvén transit time is defined by

$$\tau_A = R_0 q \left(\frac{\mu_0 \rho}{\langle B^2 \rangle} \right)^{1/2} \quad , \tag{A.11}$$

and the resistive time by

$$\tau_R = \frac{\mu_0 a^2}{\eta} \quad , \tag{A.12}$$

with ρ the plasma density on the particular surface, Q_0 and y_0 can be expressed as

$$Q_0^3 = \left[2\pi n \; a \; R_0 q \; \frac{q' \chi'}{v'} \right]^2 \frac{1}{M \langle B^2 / |\nabla s|^2 \rangle} \; \frac{1}{\tau_R {\tau_A}^2} \tag{A.13}$$

and

$$y_0^2 = \frac{1}{M \langle B^2 \rangle} \left(\frac{R_0 q \chi'}{v' \tau_A} \right)^2 \frac{1}{Q_0^2} \quad . \tag{A.14}$$

Further quantities which need specification are the mean plasma beta $\langle\beta\rangle$, here defined as

$$\langle\beta\rangle = \frac{\int\int p\sqrt{g}d\theta_p ds}{\int\int (B^2/2\mu_0)\sqrt{g}d\theta_p ds} \quad . \tag{A.15}$$

The local poloidal beta β_{AL} and the shear S_h are defined as in reference [1], namely

$$\beta_{AL} = -2\mu_0 \frac{p'v'}{\chi'^2}\sqrt{\frac{v}{2\pi^2 R_0}} \tag{A.16}$$

and

$$S_h = \frac{2v}{q}\frac{q'}{v'} \quad . \tag{A.17}$$

References

1. T. Tsunematsu et al., Data Set for Benchmark Calculation on Ideal MHD Beta Limit of INTOR Plasmas, JAERI-M, 86 - 172 (1986).

2. T. Tsunematsu et al., Japanese Contribution to Data Base Assessment, INTOR Workshop, Phase IIA, Third Part, 13th Session, March 1986, Brussels, EURFUBRU / XII-52 / 86 / EDV11.

3. L. M. Degtyarev and S. Yu. Medvedev, Influence of the INTOR Cross-section Geometry and Plasma Profiles on the Ideal MHD Beta Limits, USSR Contributions to the 14th Workshop Meeting, INTOR Phase IIA, Third Part, December 1986, Brussels / Vienna, EURFUBRU / XII - 52 / 86 / EDV23.

4. F. Troyon, European Contributions to the 13th Workshop Meeting, Physics (Groups B, C and G), INTOR Phase IIA, Third Part, March 1986, Brussels, EURFUBRU / XII - 52 / 86 / EDV10.

5. T. Tsunematsu et al., Japanese Contribution to Data Base Assessment, INTOR Workshop, Phase IIA, Third Part, 14th Session, December 1986, Brussels / Vienna, EURFUBRU / XII - 52 / 86 / EDV21 .

6. L. M. Degtyarev et al., Stability of Ideal Modes in Tokamaks, USSR Contributions to the 15th Workshop Meeting, INTOR Phase IIA, Third Part, Volume I, July 1987, Brussels / Vienna, EURFUBRU / XII - 226 /87 / EDV23.

7. T. Tsunematsu et al., Japanese Contribution to Data Base Assessment, INTOR Workshop, Phase IIA, Third Part, Volume I, 15th Session, July 1987, Brussels / Vienna, EURFUBRU / XII - 226 / 87 / EDV21.

8. F. Troyon et al., Plasma Physics 26, 209 (1984).

9. A. H. Glasser et al., Phys. Fluids 18, 875 (1975).

10. D. Correa-Restrepo, Z. Naturforsch. 37*a*, 848 (1982).

11. D. Correa-Restrepo, in Plasma Physics and Controlled Nuclear Fusion Research 1982, Vol. III, p. 519. International Atomic Energy Agency, Vienna.

12. D. Correa-Restrepo, Plasma Physics 27, 565 (1985).

13. D. Correa-Restrepo, European Contributions , INTOR Workshop, Phase IIA, Third Part, 13th Session, March 1986, Brussels, EURFUBRU / XII - 52 / 86 / EDV10.

14. A. Sykes et al., Plasma Physics 29, 719 (1987).

15. S. P. Hirshman, U. Schwenn and J. Nührenberg, Comput. Phys. Commun. (to be published).

16. U. Schwenn, private communication.

17. J. Nührenberg and R. Zille. Private communication and 12th European Conference on Controlled Fusion and Plasma Physics, Budapest, September 1985.

18. J. W. Connor et al., in Plasma Physics and Controlled Nuclear Physics Research 1982, Vol III, p. 403. International Atomic Energy Agency, Vienna.

19. H.P. Zehrfeld and K. Grassie, Resistive Ballooning Stability of ASDEX Equilibria (Report IPP 5/16, Max-Planck-institut für Plasmaphysik, D-8046 Garching, 1987).

20. G. Becker et. al., Nucl. Fusion 27, 1785 (1987).

Figure Captions

Fig. 1 Plasma cross-section and equilibrium parameters of the ideally marginally stable INTOR plasma described in Section 3.2.

Fig. 2 Safety factor q, pressure p and pressure gradient dp/ds for the equilibrium of Section 3.2. Also given is the shear versus poloidal beta diagram.

Fig. 3 Stability diagram $\Delta' > \Delta_c(n)$, Mercier exponent s_M, resistive interchange parameter D_R and magnetic Reynolds number $S/S(0)$, $S(0) = 2.08 \cdot 10^9$ corresponding to an equilibrium with $\langle\beta\rangle = 2.70\%$, calculated with the same parameters as in Fig. 1, *except for* m_0, which is here $m_0 = 0.026$.

Fig. 4 Profiles and parameters of the equilibrium defined by equations (3.3) and (3.6), with $m_0 = 0.0155$ and $\langle\beta\rangle = 2.00\%$. The plasma cross-section is similar to that in Fig. 1.

Fig. 5 Stability diagram $\Delta' > \Delta_c(n)$, Mercier exponent s_M, resistive interchange parameter D_R and magnetic Reynolds number $S/S(0)$, $S(0) = 2.66 \cdot 10^9$ for the equilibrium of Fig. 4.

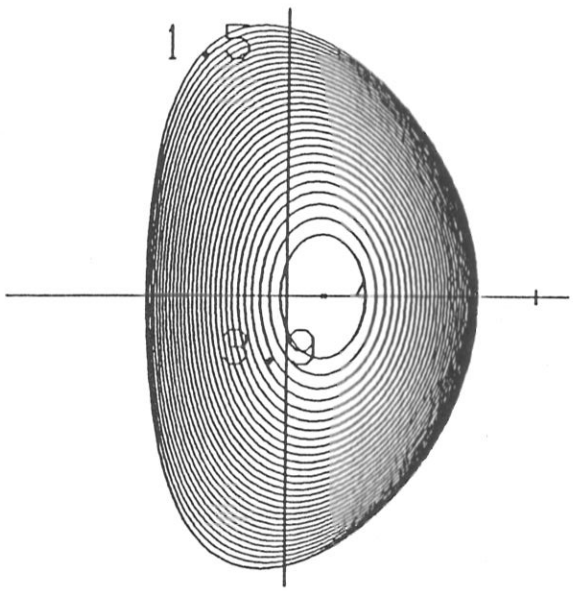

$R_0 = 4.0m$

$R_A = 4.08m$

$a = 1.0m$

$e = 1.6$

$\delta = 0.3$

$q_0 = 1.1$

$q_a = 3.1$

$m_0 = 0.029$

$\langle\beta\rangle = 3.01\%$

$B_0 = 5.5T$

$T_0 = 15keV$

Fig. 1

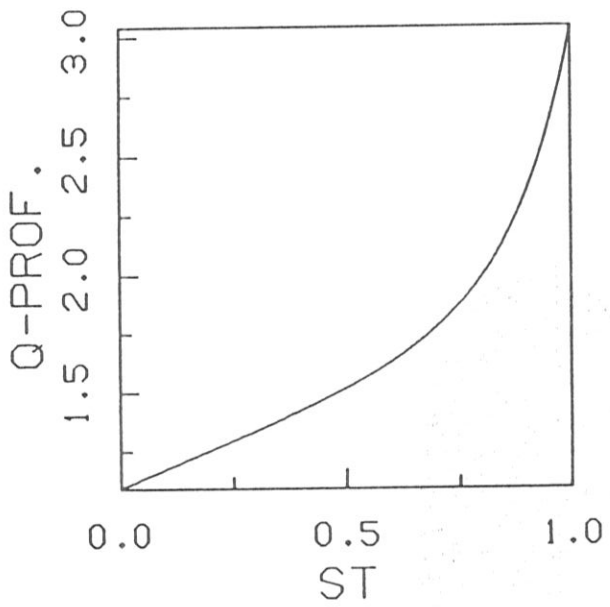
Q-PROF.
1.5
2.0
2.5
3.0
0.0
0.5
1.0
ST

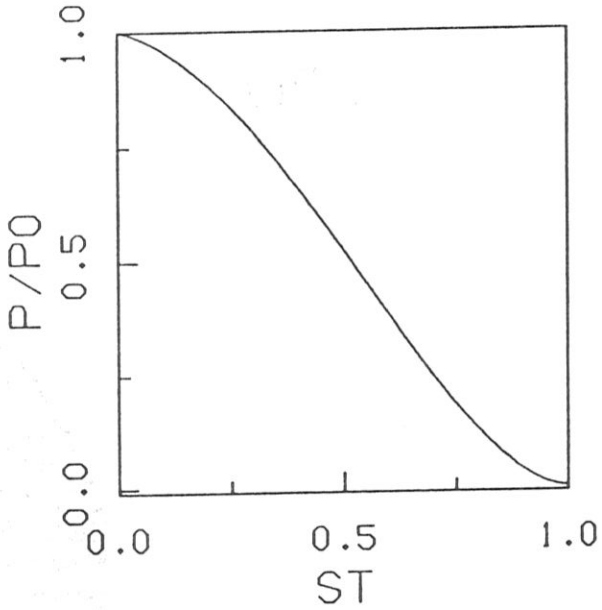
P/P0
0.0
0.5
1.0
0.0
0.5
1.0
ST

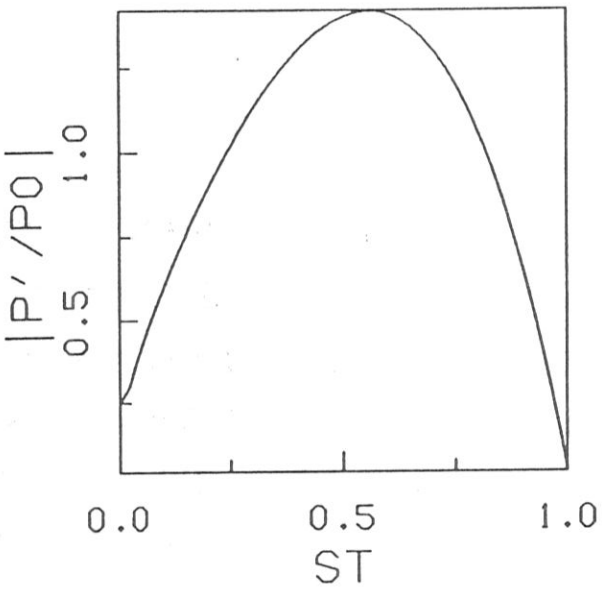
|P'/P0|
0.5
1.0
0.0
0.5
1.0
ST

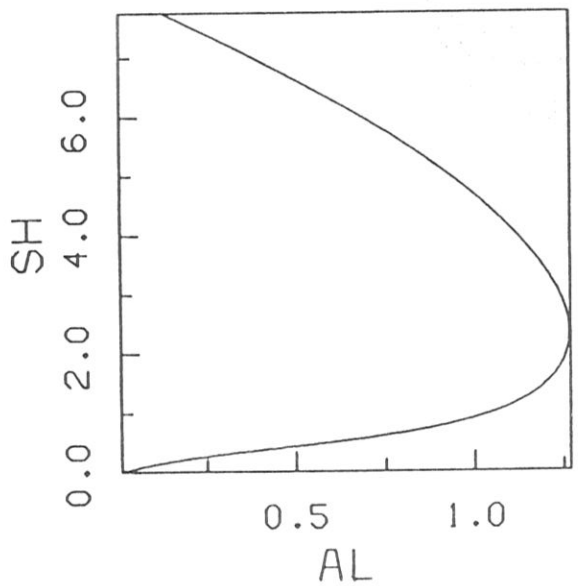
SH
0.0
2.0
4.0
6.0
0.5
1.0
AL

Fig. 2

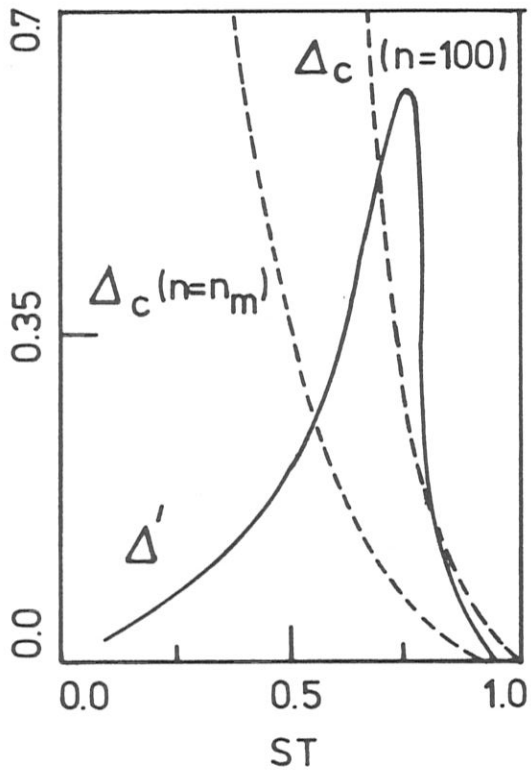
0.7
0.35
0.0
Δ_c (n=100)
$\Delta_c(\tilde{n}=n_m)$
Δ'
0.0
0.5
1.0
ST

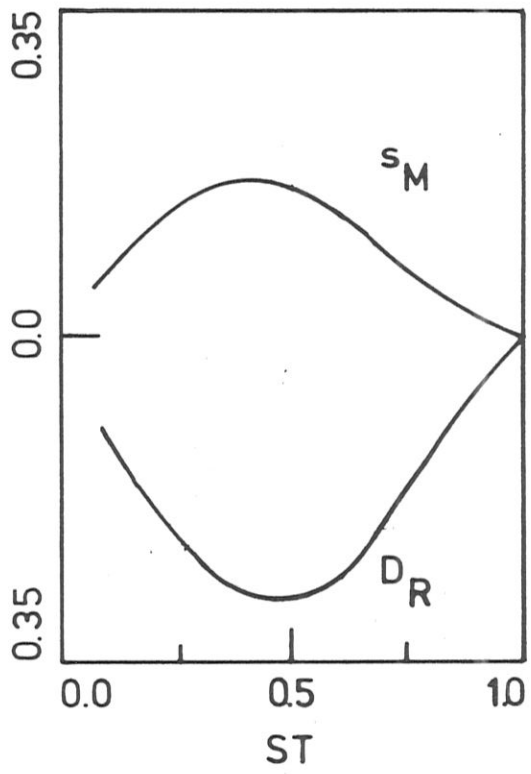
0.35
0.0
0.35
s_M
D_R
0.0
0.5
1.0
ST

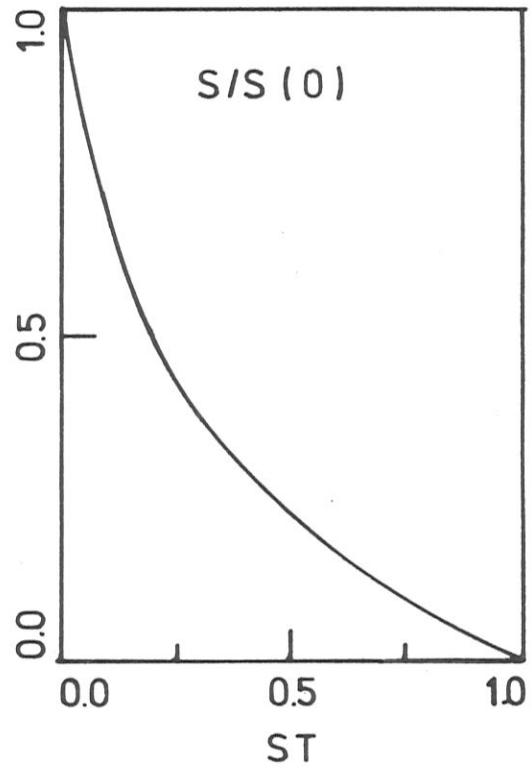
1.0
0.5
0.0
S/S (0)
0.0
0.5
1.0
ST

Fig. 3

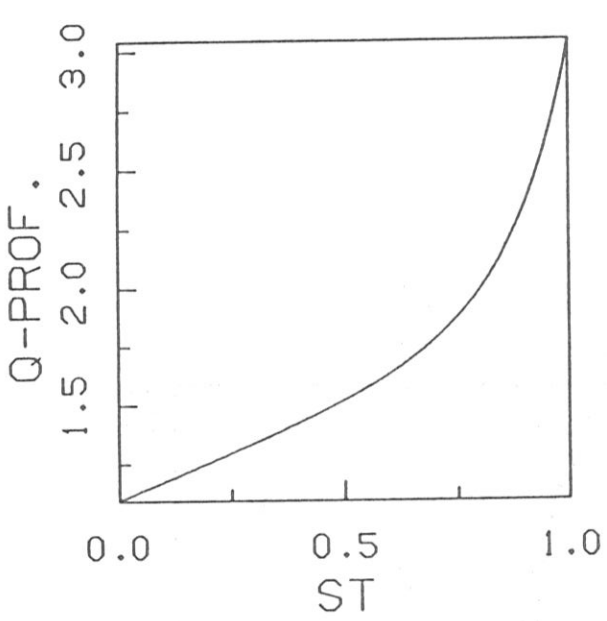
Q-PROF.
1.5
2.0
2.5
3.0
0.0
0.5
1.0
ST

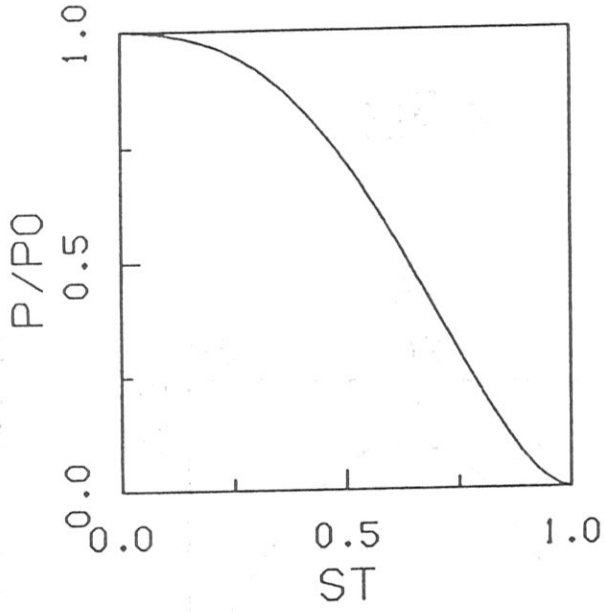
P/P0
0.0
0.5
1.0
0.0
0.5
1.0
ST

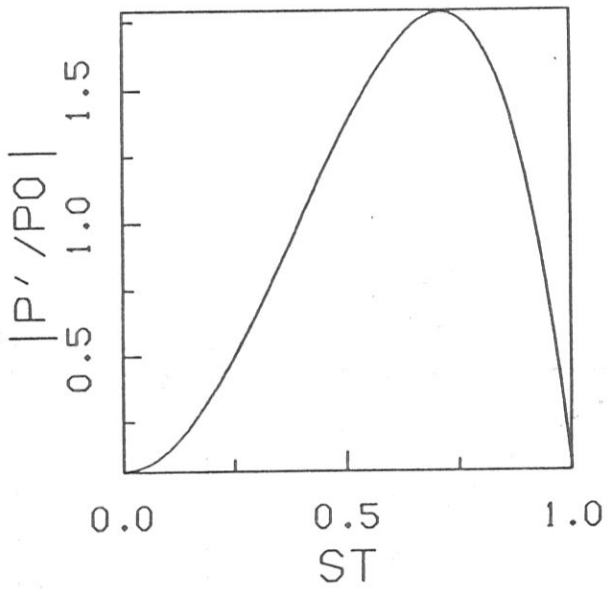
|P'/P0|
0.5
1.0
1.5
0.0
0.5
1.0
ST

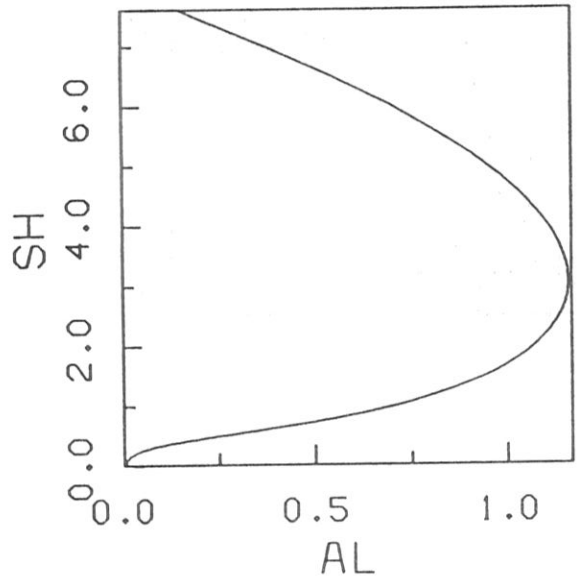
SH
0.0
2.0
4.0
6.0
0.0
0.5
1.0
AL

Fig. 4

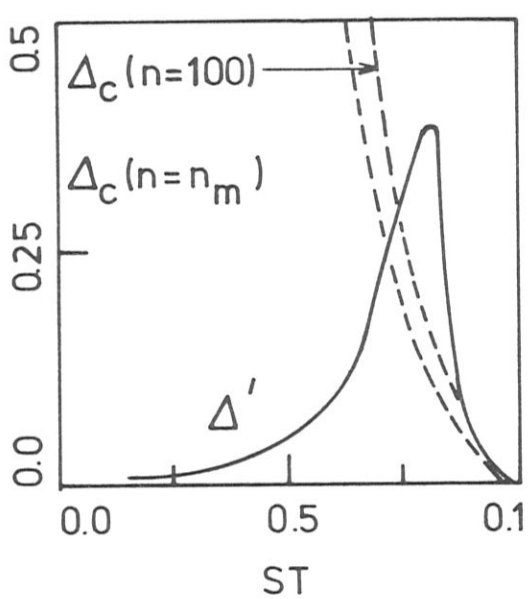
0.5
0.25
0.0
Δ_c (n=100)
Δ_c (n=n_m)
Δ'
0.0
0.5
0.1
ST

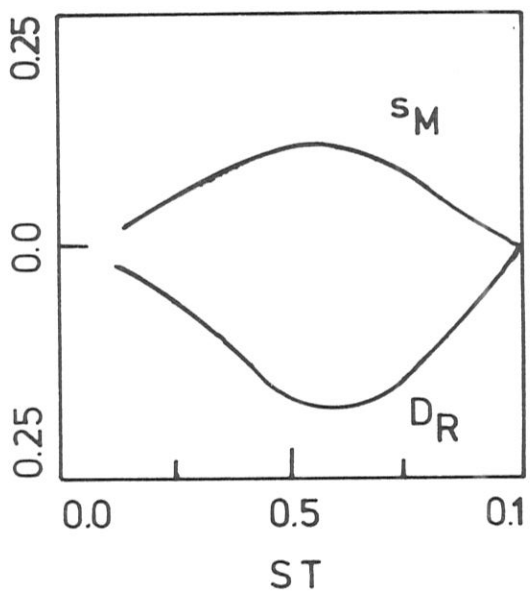
0.25
0.0
0.25
s_M
D_R
0.0
0.5
0.1
ST

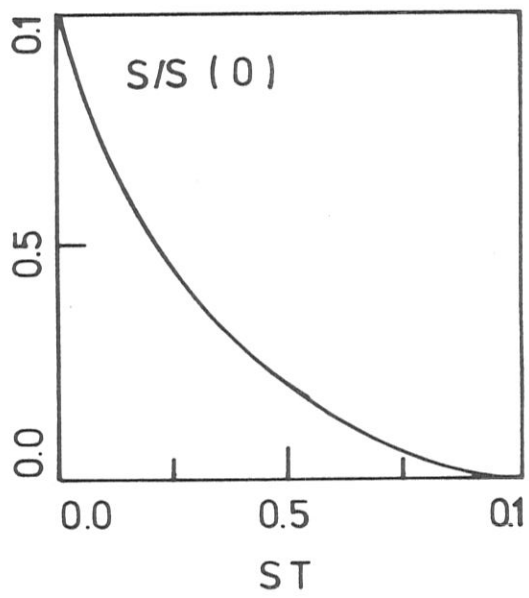
0.1
0.5
0.0
S/S (0)
0.0
0.5
0.1
ST

Fig.5